International Journal of Engineering Research & Technology (IJERT)
ISSN: 2278-0181
Vol. 4 Issue 12, December-2015

Thermal Design and Analysis of Heat Sink Optimization and its Comparison with Commercially Available Heat Sink

Pawar Shreekant Prabhakar
Department of Mechanical Engineering
Matoshri College of Engineering and research
Nasik, India

Prof. Ghuge N. C
Department of Mechanical Engineering
Matoshri College of Engineering and research
Nasik, India

***Abstract*— Modern portable electronic devices are becoming more compact in space, The exponential increase in thermal load in air cooling devices require the thermal management system (i.e. heat sink) to be optimized to attain the highest performance in the given space.**

In this work, experimentation is performed for high heat flux condition. The heat sink mounted on the hot component for cooling the component under forced convection. The two different orientation of fan i.e. "fan-on-top" and "fan-on-side" are tested for different air mass flow rate and cooling rate is validated with numerical results for the same amount of heat flux. The numerical simulation are performed using computational fluid dynamics (CFD).

The primary goal of this work is to do the thermal analysis and comparison of fan orientation on cooling efficiency and to find the optimum parameters for a natural air-cooled heat sink at which the system will continue its operation in natural convection mode (i.e. Fan-failed condition). The CFD simulations are performed for optimization of heat sink parameters with objective function of maximization of heat transfer coefficient.

Keywords*— Heat Sink, Experimental Testing, Computational Fluid Dynamics, Heat Transfer Coefficient

INTRODUCTION

It is observed that components of modern portable electronic devices with increasing heat loads with decrease in the space available for heat dissipation. The increasing heat load of the device needs to be removed otherwise overheating situation could affect both the stability and performance of the working device. The exponential increase in thermal load in air cooling devices requires the thermal management system (i.e. heat sink) to be optimized to attain the highest performance in the given space.

Over the past few decades there is increasing interest in the development of the heat sink process for heat dissipation and many design methodologies regarding optimization of heat sink have been proposed. Kyoungwoo Park [1] used Kriging method and CFD tool to an optimization of heat sink. Matthew B. de. Stadler [2] figure out difficulty in using fixed temperature boundry condition for hot surfaces and role of cellular materials while optimization of heat sinks. Some unknown [3] Characterize the performance of several fan heat sink designs and find out a theoretical methodology that would accurately predict both optimization point for a given space as well as the performance of the solution. Dong-Kwon Kim [4] check the thermal performance of plate fin heat sink with variable fin thickness and observes thermal resistance was reduced as much as 15 % compared to uniform fin thickness heat sink. Adriano A.Koga.*et.al* [5] proposed development of heat sink device by topology optimization. Sidy Ndao *et.al* [6] concluded from multi objective thermal design optimization and comparative analysis of electronic cooling technologies that Single objective optimization of either the thermal resistance or pumping power may not necessarily yield optimum performance. The multiple-objective optimization approach is preferable as it provides a solution with different trade-offs among which designers can choose from to meet their cooling needs. The choice of a coolant has a significant effect on the selection of a cooling technology for a particular cooling application. Chayi-Tsong Chen, and Hung-I Chen observed that direction based genetic algorithm is very effective in locating the pareto front of the multi objective design The optimally designed heat sink by the proposed approach is shown to be superior in heat dissipation than those reported in literature. Lin Lin *et.al* [7] observes Increasing the pumping power, Volumetric flow rate or Pressure drop can enhance the cooling performance of double layer MCHS , however this enhancement effect becomes weaker at higher pumping powers ,volumetric flow rates, and pressure drops. Paulo Canhoto and A Heitor Reis[8] address the optimization of a heat sink formed by parallel circular ducts or non circular ducts in a finite volume and found that The optimum dimensionless thermal length and optimum hydraulic diameter were found for achieving maximum heat transfer density at fixed pumping power. Dong-Kwon Kim *et.al* [9] shown that optimized pin-fin heat sinks possess lower thermal resistances than optimized plate-fin heat sinks when dimensionless pumping power is small and the dimensionless length of heat sinks is large. On the contrary, the optimized plate-fin heat sinks have smaller thermal resistances when dimensionless pumping power is large and the dimensionless length of heat sinks is small. R.Mohan and Dr. P. Govindrajan [10] did thermal analysis of CPU with pin fin and slot parallel plate heat sinks with copper and carbon carbon composites. Ravi Kandasamy *et.al* [11] investigated application of novel PCM package for thermal management of portable electronic devices experimentally for studying effect of various parameters under cyclic steady condition. Maciej Jaworski [12] address

thermal performance of heat spreader for electronic cooling with incorporated phase change materials.
In this work experimentation is performed to find out better orientation of fan and no fan(Fan failed) condition the results of the experiment are validated by CFD .The objective of this work is to find out optimum parameters for naturally air cooled heat sink at which the system will continue its operation smoothly in natural convection mode. And comparisons of optimized heat sink with commercially available heat sink on the basis of various thermal and geometrical properties.

Experimental Set-up

Fig.1 represents the experimental testing set up which consist of a 80mm×60mm plate heater attached below the heat sink using a thin layer of thermal conducting paste Omegatherm201.This attachment reduces the contact resistance and air gap between the surfaces, thus enhancing thermal conductivity during heat transfer. The heater can provide input power up to 80W to simulate the heat source. An adjustable DC power supply is connected to the heater. The maximum voltage across heater is 24V DC.

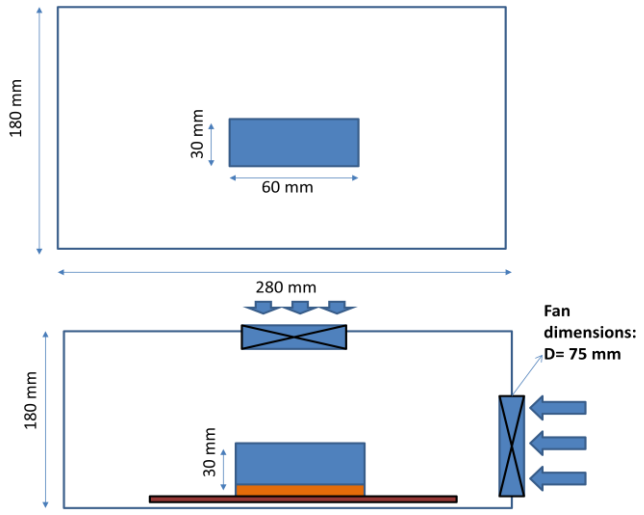

Fig.1. Front view of experimental set up

The heat sink with attached heater is enclosed in a cabinet (280X150X180) and made of 5 mm thick acrylic, which has a melting temperature of 170°C and a thermal conductivity of 0.2W/mK. Two axial fans of SIBAS (V=220 V, I=0.09 A, P=17 W, N=2500 rpm) are screwed to the cabinet casing out of which first one is mounted the top side of the heat sink and second one on right side in order to enhance the heat transfer. The heater is insulated from the casing using a backllite plate of 10 mm thickness followed by mica sheet of 1 mm thickness and ceramic wool of 10 mm thickness. This prevents heat loss from the heater to the acrylic plastic casing. To study the natural convection phenomenon inside the test set up, upper surface has not given any insulation. Rubber 'O' rings are placed on the both sides of the heat sinks before the device is sealed with M3 screws and epoxy. The metal screws hold the heat-transferring blocks tightly to the aluminum heat sink in order to avoid the contact resistance due to air gap. The setup is placed inside a black box to reduce environmental effects due to lights, flows from air-conditioning fans and other disturbance.
Four omega-type thermocouples are used for testing. First thermocouple is attached around the external surface of the heat sink. Second thermocouple is attached in between the heater and the heat sink. Third and fourth thermocouples are placed inside the cabinet near to the fans. The second end of each thermocouple is dipped in an ice bath for thermocouple calibration.

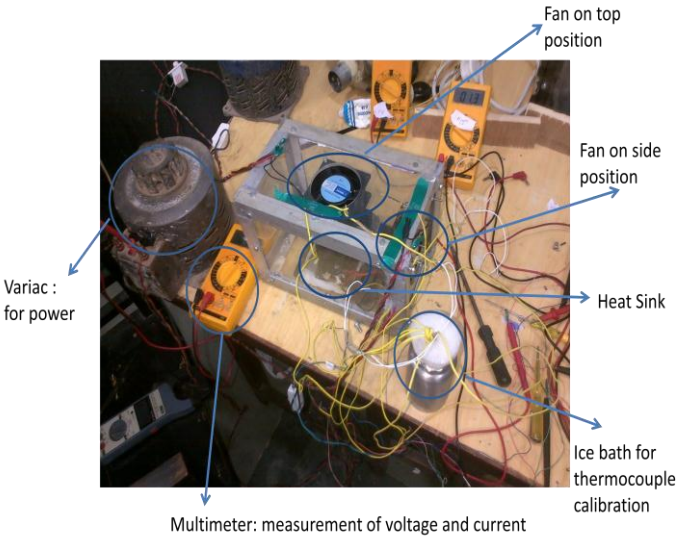

Fig. 2. Experimental set up

The opposite end of each thermocouple is attached to multimeter in order to record the temperature of each thermocouple.

Experimentation

The experiment is performed in following steps
In this experiment the readings are taken for three main conditions i.e fan on side (FOS), fan on top (FOT) and no fan (fan failed) condition.

FAN ON SIDE (FOS) CONDITION

(a) Different heat inputs are given to the heater through power source.
(b) Variac is used to regulate power supply and for giving different heat inputs.
(c) The temperature across the components is recorded after steady state is reached.
(d) The experimentation is performed for the above mentioned conditions with varying mass flow rate of air regulating the speed of fan on side.

FAN ON TOP (FOT) CONDITION

(a) Different heat inputs are given to the heater through power source.
(b) Variac is used to regulate power supply and for giving different heat inputs.
(c) The temperature across the components is recorded after steady state is reached.
(d) The experimentation is performed for the above mentioned conditions with varying mass flow rate of air regulating the speed of fan on top.

NO FAN (FAN FAILED) CONDITION

(a) Different heat inputs are given to the heater through power source.
(b) Variac is used to regulate power supply and for giving different heat inputs.
(c) The temperature across the components is recorded after steady state is reached.
(d) For this case no fan is working and the readings are taken for natural convection.

Thermal Design

For 65 W Readings

For many reasons fan less applications are getting more and more attention, simple direct adopting of market available heat sinks is no longer feasible. A clear understanding on natural convection heat transfer and how this theory can be applied to component level and system level thermal solution design is crucial.

In natural convection, where the velocity of moving air is unknown, there is no single velocity analogous to the free stream velocity that can be used to characterize the flow. Thus, we cannot use the Reynolds number in the computation. Instead, use the Grashof number to correlate natural convection flows. The Grashof number is defined as follows:

$$Gr = \frac{g\beta\rho^2(T_s - T_f)L^3}{\mu^2}$$

g = acceleration of gravity (m/s2)
β = volume expansivity= (1/K)
ρ = density of fluid (kg/m3)
Ts = surface temperature (K)
Tf = 25˚C ; 25 + 273=298 (K)
L = 0.06 m
$\mu = 1.983 * 10^{-5}$ N-S/m^2

$$Gr = \frac{9.81*2.9282*10^{-3}*(112-25)*(0.06^3)*(1.02^2)}{(1.983*10^{-5})^2}$$

$$Gr = 1.428228*10^6$$

Grashof number is a dimensionless number in fluid dynamics and heat transfer which approximates the ratio of the buoyancy to viscous force acting on a fluid. At higher Gr the boundary layer is turbulent while at lower Gr the Boundary layer is laminar.

For Calculating Prandtl no.

$$Pr = \frac{\mu}{C_{pK}}$$

$$Pr = \frac{1.983*10^{-5}*1005}{0.029}$$

$$Pr = 0.687212$$

From the values of Gr. And Pr.

$$Ra = Gr*Pr$$

$$Ra = 1.428228*10^6 * 0.687212$$

$$Ra = 9.81495*10^5$$

Optimizing thermal performance of a natural convection thermal solution involves a much broader design consideration; determining the correct fin spacing is just a part of the process. As mentioned in the earlier section, natural convection occurs mainly due to buoyancy force. Optimal fin spacing is needed to allow airflow between fins to circulate as freely as possible. In a steady state condition analysis, one could assume that thermal solution fins are close to isothermal and optimal fin spacing can be defined with a known thermal solution volume (WxDxH) as

$$S = 2.714*\frac{L}{(Ra)^{1/4}}$$

Where:
S = optimum fin spacing
L = fin length parallel to airflow direction
Ra = Rayleigh number

$$S = 2.714*\frac{0.06}{(9.81495*10^5)^{1/4}}$$

$$S = 5.17 \text{ mm}$$

For the Optimum fin spacing the Optimum Fin thickness can be calculated by

$$t = \frac{L-S(n-1)}{n}$$

Where
t = fin thickness (mm)
L = thermal solution length/size (mm)
S = optimum fin spacing (mm)
n = number of fins/section

$$t = \frac{0.06-5.17*10^{-3}(10-1)}{10}$$

$$t = 1.347 \text{ mm}$$

The Nusselt number for the Natural convection can be calculated by using the correlation

$$Nu = 0.1*Ra^{(1/3)}$$
$$Nu = 0.1*9.81495*10^5$$
$$Nu = 10.39395$$

Convective heat transfer Coefficient

The convective heat transfer coefficient can be calculated by using the formula

$$Nu = \frac{h*L}{k}$$
$$10.39395 = \frac{h*0.06}{0.029}$$
$$h = 3.464651 \text{ w/m}^2\text{k}$$

Same as above the values of all parameters by experiment are tabulated below for 25W, 40W, 65W.

Sr.No.	P (W)	Gr	Pr	Ra	S (mm)	t (mm)	Nu	h (w/m^2k)
01	25	1.22*10^6	0.68721	838950.6	5.381	1.158	9.431457	3.143819
02	40	1446182	0.68721	993833.8	5.157	1.358	9.979404	3.326468
03	65	1633998	0.68721	1122903	5.002	1.498	10.39395	3.464651

Computational Fluid Dynamic Study

Governing Equations of Fluid Flow

The most general form of fluid flow and heat transfer equations of compressible

Newtonian fluid with time dependency is given as follows:

Continuity Equation: $\frac{\partial \rho}{\partial t}+\frac{\partial(\rho u)}{\partial x}+\frac{\partial(\rho v)}{\partial y}+\frac{\partial(\rho w)}{\partial z}=0$

X Momentum Equation

$\frac{\partial(\rho u)}{\partial t}+\frac{\partial(\rho u^2)}{\partial x}+\frac{\partial(\rho uv)}{\partial y}+\frac{\partial(\rho uw)}{\partial z}=-\frac{\partial p}{\partial x}+\frac{1}{Re}[\frac{\partial \zeta_{xx}}{\partial x}+\frac{\partial \zeta_{xy}}{\partial y}+\frac{\partial \zeta_{xz}}{\partial z}]$

Y Momentum Equation

$\frac{\partial(\rho v)}{\partial t}+\frac{\partial(\rho uv)}{\partial x}+\frac{\partial(\rho v^2)}{\partial y}+\frac{\partial(\rho vw)}{\partial z}=-\frac{\partial p}{\partial y}+\frac{1}{Re}[\frac{\partial \zeta_{xy}}{\partial x}+\frac{\partial \zeta_{yy}}{\partial y}+\frac{\partial \zeta_{yz}}{\partial z}]$

Z Momentum Equation

$\frac{\partial(\rho w)}{\partial t}+\frac{\partial(\rho uw)}{\partial x}+\frac{\partial(\rho vw)}{\partial y}+\frac{\partial(\rho w^2)}{\partial z}=-\frac{\partial p}{\partial z}+\frac{1}{Re}[\frac{\partial \zeta_{xz}}{\partial x}+\frac{\partial \zeta_{yz}}{\partial y}+\frac{\partial \zeta_{zz}}{\partial z}]$

Energy Equation $\frac{\partial(E_T)}{\partial t}+\frac{\partial(uE_T)}{\partial x}+\frac{\partial(vE_T)}{\partial y}+\frac{\partial(wE_T)}{\partial z}=-\frac{\partial(up)}{\partial x}-\frac{\partial(vp)}{\partial y}-\frac{\partial(wp)}{\partial z}-\frac{1}{RePr}\left[\frac{\partial q_x}{\partial x}+\frac{\partial q_y}{\partial y}+\frac{\partial q_z}{\partial z}\right]+\frac{1}{Re}[\frac{\partial}{\partial x}(u\zeta_{xx}+v\zeta_{xy}+w\zeta_{xz})+\frac{\partial}{\partial y}(u\zeta_{xy}+v\zeta_{yy}+w\zeta_{yz})+\frac{\partial}{\partial z}(u\zeta_{xz}+v\zeta_{yz}+w\zeta_{zz})]$

Set of equations are solved using pressure based model. Staggered grid arrangement is taken for study. For pressure velocity coupling SIMPLE algorithm is considered. Second order upwind scheme is considered for descretising the momentum equation. For turbulence modeling K-E model is considered. For meshing the geometry, fine sgrid is used to near Fan, velocity boundary layer is need to be captured for getting accurate profile. Fine grid is also used near heat sink fins in order to capture thermal boundary layer. In rest of the domain where physics change is not prominent, coarse grid is used to save computational time.

CFD Modelling

Turbulent model

- K-epsilon (k-ε) turbulence model is the most common model used in Computational Fluid Dynamics (CFD) to simulate mean flow characteristics for turbulent flow conditions.
- It is a two equation model which gives a general description of turbulence by means of two transport equations (PDEs).
- The original impetus for the K-epsilon model was to improve the mixing-length model, as well as to find an alternative to algebraically prescribing turbulent length scales in moderate to high complexity flows.
- The first transported variable determines the energy in the turbulence and is called turbulent kinetic energy.
- The second transported variable is the turbulent dissipation which determines the rate of dissipation of the turbulent kinetic energy.

CFD model- Fan on side condition

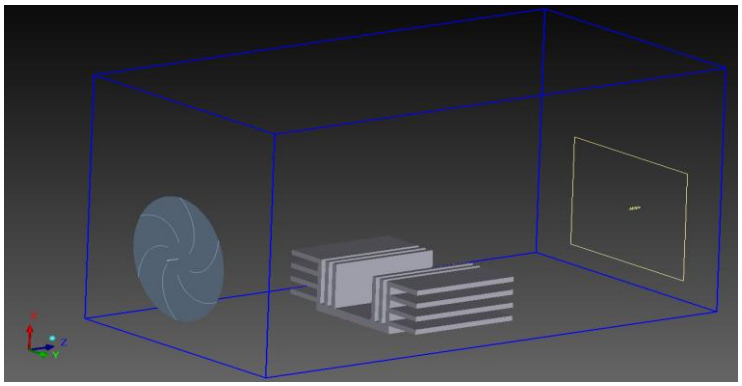

Figure 3 CFD model FOS Condition

CFD model- Fan on top condition

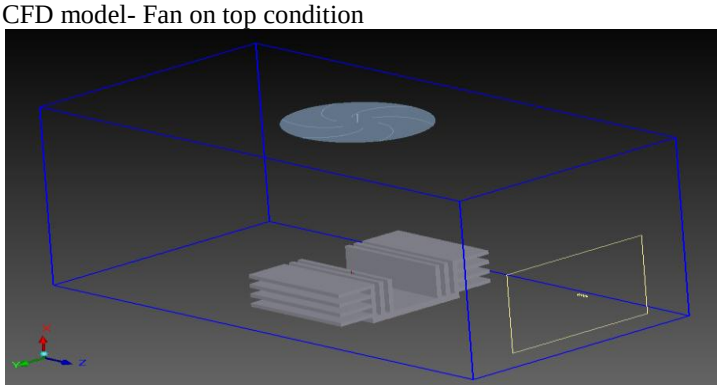

Figure 4 CFD model FOT Condition

Grid Generation / Meshing

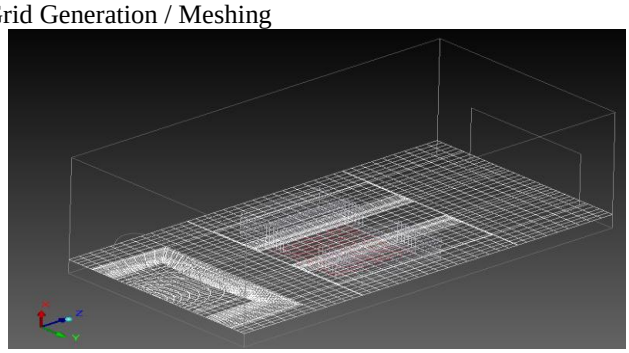

Figure5 Meshing in X Plane

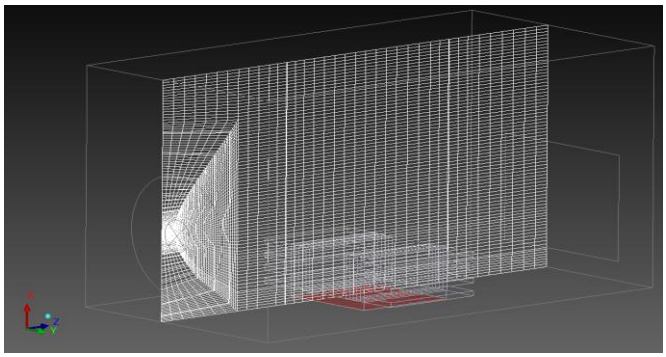

Figure.6 Meshing in Y Plane

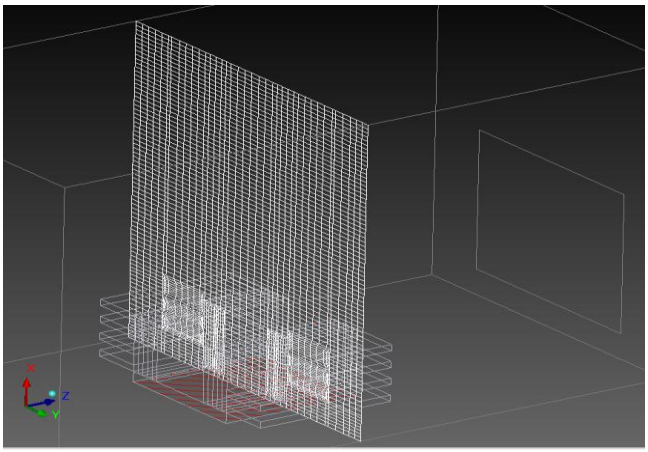

Figure.7 Meshing in Z Plane

- Grid Clustering is used i.e. find at the location where most drastic change in physics is occurred
- Fine grid is used to near Fan, velocity boundary layer is need to be captured for getting accurate profile.
- Fine grid is also used near heat sink fins in order to capture thermal boundary layer.
- In rest of the domain where physics change is not prominent, coarse grid is used to save computational time.

Results and Discussion

COMPARISION OF HEAT SINK TEMPERATURE FOR DIFFERENT FAN ORIENATION AND POWER INPUTS

The Temperature readings obtained from experiment and CFD for both orientations of fan (i.e FOS and FOT) and varying mass flow rate of air are plotted. The graphs for input power 25 W and 65 W clearly observed that experimental readings show much similarity with CFD results with minor deviation. The Graph also indicate that temperature readings obtained at the fin tip in case of fan on side (FOS) condition is much lower than fan on top (FOT) condition. These results are very useful for selecting the orientation of fan for electronic cooling with respect to position of heat sink.

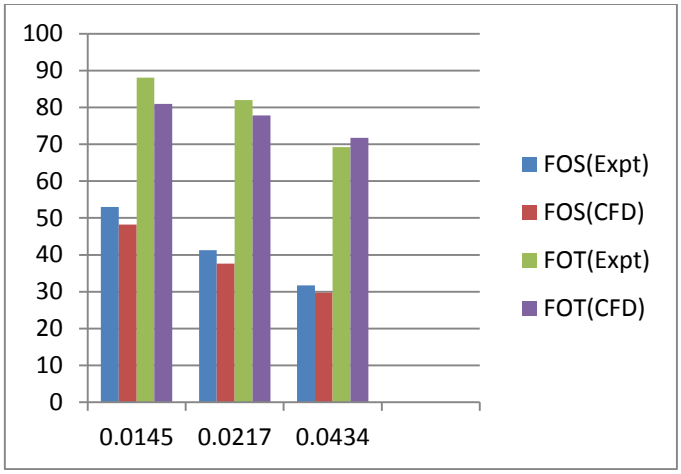

Figure 8.Comparison of heat sink temperature for different orientation of fan for 25 W

For 65 W

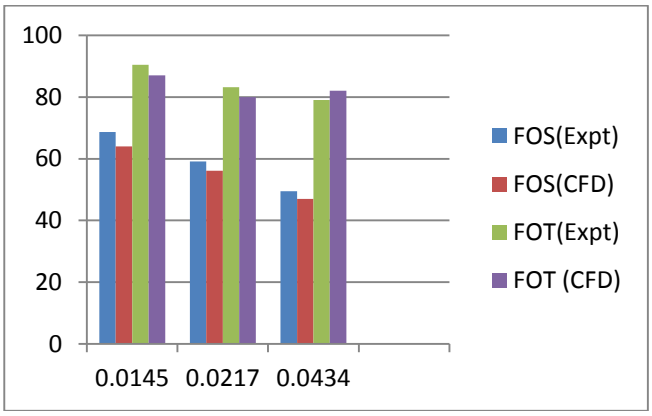

Figure 9Comparison of heat sink temperature for different orientation of fan for 65W

Fan Failed Condition

COMPARISON OF HEAT SINK TEMPERATURE (BASE CASE) WITH IGBT PERMISSIBLE TEMPERATURE

The input power is plotted against IGBT permissible temperature and temperature reading obtained in experiment for fan failed condition. The graph for said condition clearly shows that the experimental readings of temperature as well as the CFD readings for fan failed condition exceeds IGBT Temperature .the graph concludes the need of optimizing given heat sink.

Figure.10.Comparison of heat sink temperature with IGBT permissible temperatures

EFFECT POWER INPUTS ON VARIATION OF OPTIMIZED FIN THICKNESS AND FIN SPACING

The effect of variation of optimized fin thickness and optimized fin spacing with respect to different input powers. It can be noted from the graph that when fin thickness is reduced at the same time fin spacing goes on increasing. Also when fin spacing is reduced at that time fin thickness needs to be increased for dissipating the required amount of heat load from the given heat sink. The graph also shows the good agreement of experimental results with CFD validated results. From this study the optimum Fin spacing is 5.17mm and optimum fin thickness is 1.3147mm .both parameters can be approximated as spacing is 5mm and thickness as 1.5 mm for easy manufacturing of heat sink

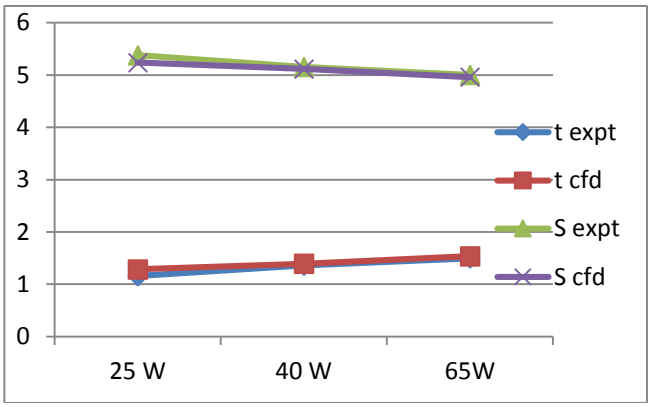

Figure11.Variation of optimized fin spacing and thickness with different input powers

COMPARISON OF HEAT SINK TEMPERATURE FOR VARIOUS CASES

The optimized results in terms of temperature for all the cases and for No fan (Fan failed) condition are given below

Table 2 Temperatures for different configurations of heat sink

Input Power(W)	Heat Sink Temperatures (℃)			
	Base Case	Case-I	Case-II	Case-III
25	90	84	64	53
65	112	111	95	90.5

Same results are represented graphically. In this red line shows permissible temperature limit for given IGBT.

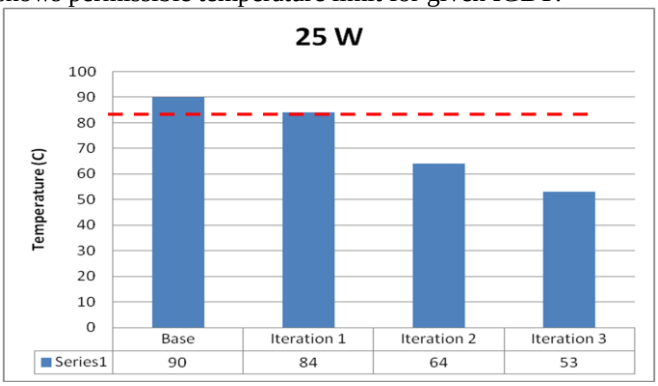

Figure 12. Heat sink temperatures for different configurations of heat sink at 25 W

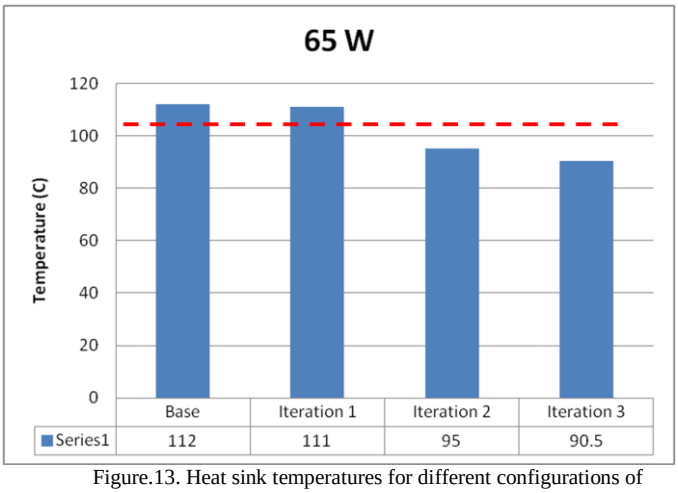

Figure.13. Heat sink temperatures for different configurations of heat sink at 65 W

From the above results it is clear that case II is the best optimized condition for given heat sink setup.

COMPARISON OF CONVECTIVE HEAT TRANSFER COEFFICIENT AT DIFFERENT INPUT POWERS IN EXPERIMENT AND IN CFD

The graph of comparison of heat transfer coefficient in experiment and in CFD is plotted against the input powers. The graph clearly shows the heat transfer coefficient is increases with increase in heat supplied to heat sink. Also the graph shows the increase of heat transfer coefficient for CFD value is more than the experimental value this is due to various assumptions made in CFD study.

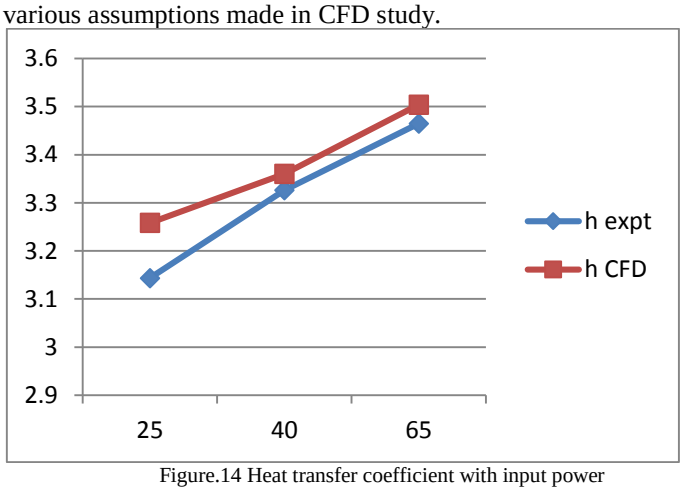

Figure.14 Heat transfer coefficient with input power

Conclusion

In this study, CPU cooling has been investigated in the acrylic cabinet with chosen heat sink and the performance of the heat sink is investigated experimentally and then validated using CFD. A road map has been developed for simulating the computer chassis. The mesh resolution, turbulence model choice, convergence criteria and discretization schemes are investigated to find the best model with least computational expense. This road map is then applied for different heat sink geometries and the comparison of the heat sink temperature difference results were made with the available experimental results. The numerical methods showed agreement with the experimental data. However, the comparison was qualitative. In order to make better comparisons, the experiment should be performed on a

computer chassis considering the full model. In this study, since it is not feasible to model the optimized heat sink and resistances with their exact geometry, lumped parameter models are used.

From the Figure 8 and 9 it is clear that for forced convection cooling fan on side orientation gives the better results than fan on top orientation. Also when the same results are validated using CFD study then it shows better agreement with experimental results.

Graph 10 shows for fan failed condition, when temperature of heat sink is compared with IGBT permissible temperatures at different input powers. It can be observed that for the said condition the heat sink temperature exceeding the IGBT permissible temperature.

Graph 12 and 13 compares heat sink temperatures of different configurations. The graph clearly shows for case-I the heat sink temperature exceed the IGBT permissible value. Case-II, Case-III shows heat sink temperatures are well within IGBT permissible range. And Case-II gives best combination of optimized heat sink for given set up.

ACKNOWLEDGMENT

I wish to express my sincere gratitude to my guide Prof. N. C. Ghuge for guidance and help which had gone a long way in the process of completion of this paper . I would also like to thank Prof D. D. Palande for his support and guidance.

REFERENCES

[1] Kyoungwoo Park., Park-Kyoun oh., Hyo-Jae Lim., The application of the CFD and Kringing method to an optimization of heat sink, International Journal of Heat and Mass Transfer 49 (2006) 3439-3447 ,Elsevier 2006.

[2] Matthew B. de Stadler., Optimization of the geometry of a heat sink, university of Virginia, Charlottesville, VA22904

[3] Kim D., Jung J., Kim S.,Thermal optimization of plate-fin heat sinks with variable fin thickness, International Journal of Hear and Mass Transfer 53(2010) 5988-5995,Elseveir,2010.

[4] Koga A., C Edson., Nova H., Lima C., Silva E., Development of heat sink by using topology optimization , International Journal of Hear and Mass Transfer 64 (2013) 759-722

[5] Ndao S., Peles Y., Jenson M.K., Multi-objective thermal design optimization and comparative analysis of electronics cooling technologies, International Journal of Hear and Mass Transfer 52 (2009) 4317-4326, Elseveir, 2009.

[6] Tsong C.,and Chen H.,Multi-objective optimization design of plate fin heat sink using a direction based genetic algorithm,Journal of the Taiwan Institute of chemical Engineers 44(2013) 257-265 Elesevier 2013

[7] Lin Lin, Yang Yang Chen ,Optimization of geometry and flow rate distributin for double layer microchannel heat sink,International journal of Thermal Sciences 78(2014 158-168 ELSEVIER

[8] anhoto P., Reis A., Optimization of forced convection heat sinks with pumping power requirements , International Journal of Hear and Mass Transfer 54 (2011) 1441-1447,Eleseveir 2010. “PDCA12-70 data sheet,” Opto Speed SA, Mezzovico, Switzerland.

[9] Kim D., Jung J., Kim S.,Thermal optimization of plate-fin heat sinks with variable fin thickness, International Journal of Hear and Mass Transfer 53(2010) 5988-5995,Elseveir,2010.

[10] R.Mohan and Dr.P.Govindrajan., Thermal analysis of CPU with Composite pin fin heat sinks, International journal of engineering science and technology vol2(9),2010,4051-4062

[11] S.C.Fok, W. Shen, F.L.Tan., Cooling of portable hand held electronic devices using phase change materials in finned heat sinks, International journal of thermal sciences 49(2010) 109-117,Elsevier, 2009.

[12] S P Pawar and N C Ghuge Design and analysis of heat sink optimization and its comparison with commercially available heat sink , M-17 Mech PGCON 2015